Journal Pre-proof

Saikosaponin B2 attenuates kidney fibrosis via inhibiting the Hedgehog Pathway

Dadui Ren , Jia Luo , Yingxue Li , Jing Zhang , Jiahong Yang , Junqiu Liu , Xuemei Zhang , Nengneng Cheng , Hong Xin

Please cite this article as: Dadui Ren , Jia Luo , Yingxue Li , Jing Zhang , Jiahong Yang , Junqiu Liu , Xuemei Zhang , Nengneng Cheng , Hong Xin , Saikosaponin B2 attenuates kidney fibrosis via inhibiting the Hedgehog Pathway, *Phytomedicine* (2019), doi: https://doi.org/10.1016/j.phymed.2019.153163

This is a PDF file of an article that has undergone enhancements after acceptance, such as the addition of a cover page and metadata, and formatting for readability, but it is not yet the definitive version of record. This version will undergo additional copyediting, typesetting and review before it is published in its final form, but we are providing this version to give early visibility of the article. Please note that, during the production process, errors may be discovered which could affect the content, and all legal disclaimers that apply to the journal pertain.

Saikosaponin B2 attenuates kidney fibrosis via inhibiting the

Hedgehog Pathway

Dadui Ren[a,#], Jia Luo[a,#], Yingxue Li[a], Jing Zhang[a], Jiahong Yang[a], Junqiu Liu[b], Xuemei Zhang[a],

Nengneng Cheng[a,*], Hong Xin[a,*]

[a] *Department of Pharmacology, School of Pharmacy, Fudan University, Shanghai 201203, PR China*

[b]*Laboratory of Medicinal Plant Biotechnology, College of Pharmacy, Zhejiang Chinese Medical University,*

Hangzhou, Zhejiang 310053, PR China

[*] Corresponding author at: Department of Pharmacology, School of Pharmacy, Fudan University,
Shanghai, China.
 E-mail addresses: chengnn@163.com (N. Cheng), xinhong@fudan.edu.cn (H. Xin).
 Phone number: 8613671829118 (H. Xin).
[#] These authors contributed equally to this work.

Abstract

Background: Renal interstitial fibrosis is a common pathway through which chronic kidney disease progresses to end-stage renal disease. There are currently no effective drugs available to treat kidney fibrosis, so traditional medicine is likely to be a candidate. The therapeutic potential of saikosaponin B2 (SSB2), a biologically active ingredient of Radix Bupleuri, on renal fibrosis has not been reported.

Methods: A unilateral ureteral obstruction (UUO) model was conducted to induce renal interstitial fibrosis in mice. SSB2's effect was valuated by histological staining and exploring the changes in expression of relative proteins and mRNAs. A conditional medium containing sonic hedgehog variant protein stimulating normal rat kidney interstitial fibroblast cells (NRK-49F) was used in an *in vitro* model to determine the possible mechanism. The molecular target of SSB2 was verified using several mutation plasmids.

Results: SSB2 administration reduced kidney injury and alleviated interstitial fibrosis by decreasing excessive accumulation of extracellular matrix components in UUO mice. It could also reduce the expression of α-SMA, fibronectin and Gli1, a crucial molecule of the hedgehog (Hh) signaling pathway both *in vivo* and *in vitro*. In NIH-3T3 cells simulated by conditional medium containing sonic hedgehog variant protein, SSB2 showed the ability to decrease the expression of Gli1 and Ptch1 mRNA. Using a dual-luciferase reporter assay, SSB2 suppressed the Gli-luciferase reporter activity in NIH-3T3 cells, and the IC_{50} was 0.49 μM, but had no effect on the TNF-α/NF-κB and Wnt/β-catenin signaling pathways, indicating the inhibition selectivity on the Hh signaling pathway. Furthermore, SSB2 failed to inhibit the Hh pathway activity evoked by ectopic expression of Gli2ΔN and Smo D473H, suggesting that SSB2 might potentially act on smoothened receptors.

Conclusion: SSB2 could attenuate renal fibrosis and decrease fibroblast activation by inhibiting the Hh signaling pathway.

Keywords: Saikosaponin B2; Hedgehog signaling; kidney fibrosis; Gli1; Smo receptor

Abbreviations: α-SMA, α-smooth muscle actin; NF-κB, receptor-activated nuclear factor kappa B; PBS, phosphate buffer solution; PGE2, prostaglandin E2; TNF-α, tumor necrosis factor-α; TGF-β1, transforming growth factor-β1; CPN, cyclopamine

Introduction

Renal interstitial fibrosis (RIF) is a common pathway through which chronic kidney disease (CKD) progresses to end-stage renal disease(Meran and Steadman, 2011; Vilayur and Harris, 2009). The majority of CKD cases have common pathological features, including activating relentless myofibroblast production, deposition of extracellular matrix (ECM), and progressive fibrous scar formation(Meran and Steadman, 2011; Zeisberg and Neilson, 2010). Despite the enormity of this problem, the current therapeutic options for chronic kidney disease in clinical settings are often ineffective(Decleves and Sharma, 2014).

However, the molecular mechanisms underlying interstitial fibrosis in kidney tissues are complex and not fully understood. Multiple studies have focused on transforming growth factor-β1 (TGF-β1) in the pathogenesis of progressive renal fibrosis. However, complete blockade of TGF-β1 is not sufficient to mitigate renal disease and may exacerbate the disease by intensifying inflammation(Chen et al., 2018). Hedgehog (Hh) signaling is an evolutionary conserved developmental pathway that plays an essential role in regulating mammalian embryonic development (Robbins et al., 2012). The three Hh ligands, namely, Sonic hedgehog (Shh), Indian hedgehog (Ihh) and Desert hedgehog (Dhh), are lipid-modified proteins that are capable of acting over a short and long distance from the source of secretion. Three Gli transcription factors are important in mediating Hh signaling. Gli2 and Gli3 are thought to have both activation and repression functions, whereas Gli1 only acts as an activator(Bowers et al., 2012). Recent works have shown that Hh signaling is reactivated in the kidney after injury and that it is an important mediator of progressive fibrosis(Ding et al., 2012; Fabian et al., 2012). Gli1 transcription factor, the direct downstream target and reporter of active Hh signaling, is specifically induced in renal interstitial fibroblasts of fibrotic kidneys(Ding et al., 2012). Studies have shown that the kidneys in Gli1-deficient mice are protected against the development of tubulointerstitial fibrosis after UUO(Ding et al., 2012; Rauhauser et al., 2015). Furthermore, when using cyclopamine (CPN), the smoothened receptor (Smo) inhibitor, to repress the induction of Gli1, matrix expression was reduced and fibrotic lesions was mitigated in obstructive nephropathy(Ding et al., 2012; Rauhauser et al., 2015).

The root of *Bupleurum chinensis* DC. is a commonly used traditional Chinese medicine. *Radix*

Bupleuri is a perennial herbaceous plant of Umbelliferae. Saikosaponins (SSs) are the major biologically active ingredients in *Radix Bupleuri*, and they have been found to have many pharmacological effects(Li et al., 2018). Their chemical compositions have been extensively studied; among them, saikosaponins A, B2, C, and D are commonly used in clinical practice(Kuntzen et al., 2008). Saikosaponin B2 (SSB2, Fig.1) has been studied as a combination drug in cancers(Zhao et al., 2019) and hepatitis C(Lee et al., 2019), but little research about the effect of SSB2 in kidney fibrosis has been reported. The present study examined the effect of SSB2 on renal fibrosis and the potential mechanism concerning inhibition of the Hh pathway.

Materials and Methods

Reagents, antibody and plasmids

SSB2, CPN, GDC-0449, JQ-1, BAY11-7082 and H-89 were purchased from Selleck Chemicals. The purity of all compounds was more than 99% according to the data sheet from manufacture. TNF-α and PGE2 were obtained from Sigma-Aldrich (St. Louis, MO). Antibodies against GAPDH, α-SMA, Gli1, Alexa Fluor 555 and 488, and goat anti-rabbit IgG were purchased from Cell Signaling Technology (Danvers, MA, USA), anti-fibronectin was purchased from Abcam (Cambridge, MA, USA), and anti-collagen I was purchased from ABclonal. All materials for the cell culture were obtained from Life Technologies, Inc. (GIBCO, USA). The $8 \times$ Gli1-binding site luciferase reporter ($8 \times$ GBSluciferase) plasmid was kindly provided by Dr. Hiroshi Sasaki. The TCF/LEF-luciferase reporter plasmid, NF-κB luciferase reporter plasmid, and TK-Renilla luciferase plasmid were purchased from Promega (Madison, WI). The Gli2 variant missing 328 N-terminal amino acids (Gli2ΔN) and the Shh variant containing the N-terminal signaling domain of sonic hedgehog (ShhN) were obtained from Addgene (Cambridge, MA). The mutant human plasmid Smo D473H was generated from wild-type Smo plasmids using the QuikChange Site-Directed Mutagenesis kit from Agilent (Santa Clara, CA) and confirmed by sequencing. Lipofectamine 2000 was from Invitrogen (Grand Island, NY).

Animal models

Male C57BL/6 (20-22 g) mice were obtained from Shanghai Slaccas Laboratory Animal Co., Ltd. (Shanghai, China). All study protocols were approved by the Animal Ethical Committee of the School of Pharmacy, Fudan University. Renal fibrosis was induced in the UUO model by cutting

between two ligated points of the left ureter in mice as previously described(Li et al., 2007), and sham-operated mice underwent the same procedure except for the obstruction. Mice (n = 6 per group) were randomly assigned to five groups: sham-operated, UUO-treated with vehicle, UUO-treated with different concentrations of SSB2 (15 mg/kg and 30 mg/kg per day) and UUO-treated with CPN (5 mg/kg per day). SSB2 was complexed with 2-hydroxypropyl-b-cyclodextrin dissolved in 0.9% NaCl as well as CPN as previous description(Ding et al., 2012). SSB2 was administered by daily intraperitoneal injection from 7 days before UUO, and CPN was administered one day before UUO. Seven days after surgery, the mice were sacrificed, and the left kidneys were collected for further analyses.

Cell culture and treatment

Normal rat kidney interstitial fibroblast cell lines (NRK-49F), mouse embryo fibroblast cell lines (NIH-3T3), LS174T colon cancer cells and HEK293T were purchased from ATCC (Manassas, USA). Cells were routinely cultured according to the instructions from ATCC. In brief, the NRK-49F cells were cultured at 37∘C in a humidified 5% CO_2 atmosphere in Dulbecco's modified Eagle's medium with 5% fetal bovine serum and 100 U/ml penicillin-streptomycin, and LS174T, 293T and NIH-3T3 cells were cultured with 10% fetal bovine serum. NRK-49F cells were seeded onto six-well plates with a density of 1×10^5 cells per well and maintained in complete medium overnight. After serum starvation for 16 hours the medium was changed to a serum-free medium with or without the ShhN-conditioned medium, and then different concentrations of SSB2 (5, 10, and 20 μM) or GDC0449 (100 nM) were added to the serum-free medium for 24 or 48 hours for analyses as indicated.

ShhN conditioned medium (CM) preparation

ShhN CM was prepared as previously described (Maity et al., 2005). In brief, HEK293T cells were transfected with ShhN plasmid or GFP plasmid as the control. The CM was collected after transfection of 48 hours.

Cell transfection

ShhN plasmid, Gli2ΔN plasmid, Smo D473H plasmid, Gli-luciferase reporter plasmids containing $8 \times$ Gli binding sites, luciferase reporter plasmids containing NF-κB binding sites, and luciferase reporter constructs containing TCF/LEF binding sites were prepared as indicated using

5

Lipofectamine 2000 reagent according to the manufacturer's instructions.

Dual‑luciferase reporter assay

LS174T, 293T and NIH-3T3 cells seeded in 96-well plates were transfected with luciferase reporter constructs containing TCF/LEF binding sites, luciferase reporter plasmids containing NF-κB binding sites and Gli-luciferase reporter plasmids containing $8 \times$ Gli binding sites, respectively, and TK-Renilla luciferase reporter constructs (Promega) for 36 hours, followed by various treatments as indicated for 24 hours. The luciferase activity in the cell lysates was examined with a Dual Luciferase Reporter Assay System (Promega) according to the manufacturer's instructions in a luminometer (Molecular Devices; Sunnyvale, CA). The firefly luciferase values were normalized to Renilla values.

Histological and Immunohistochemical Analysis

Seven days after surgery, the mice were sacrificed and the left kidneys were collected. A portion of each kidney was fixed overnight in 4% paraformaldehyde at 4°C and embedded in paraffin. The paraffin-embedded kidney sections were sectioned at a 4-μm thickness. The sections were deparaffinized using xylene and rehydrated using consecutive ethanol washes of 100%, 95%, 75%, and 50%. The samples were placed in PBS and stained with hematoxylin, eosin, Masson's trichrome, and Sirius red and scanned (400×). The fibrotic fraction volume ratio was expressed as the interstitial area relative to the total area. Immunohistochemical staining was performed using an established procedure. A total of 30 random fields were selected to capture images using a Carl Zeiss LSM710 confocal microscope. Images were subsequently quantified with Image Pro-Plus 6.0 software (Rockville, MD, USA).

Western blot analysis

Cell and kidney tissue extracts were prepared, proteins were separated by SDS-PAGE, and Western blotting was performed according to standard procedures. The proteins were then transferred onto polyvinyl difluoridine membranes, which were incubated overnight at 4 °C with the corresponding primary antibodies. Then, the membranes were incubated with secondary antibodies and detected by enhanced chemiluminescence (ECL) and visualized using the ChemiDoc™ Touch Imaging System (Bio-Rad, Hercules, CA, USA). Band intensity was quantified using ImageJ software and normalized to the respective control according to the

manufacturer's instructions.

Real-time RT-PCR

Total RNA of the cells or kidney tissues was extracted using Trizol (TAKAR, AJapan) according to the manufacturer's instructions. The RNA concentration and purity were assessed using a TECAN infinite M200PRO spectrophotometer. Total RNA was reverse-transcribed using PrimeScriptTM RT Master Mix (perfect Real Time; Takara, Japan). Each complementary DNA sample was analyzed in triplicate with a BIO-RAD CFX Connect Real-time PCR system using SYBR Premix Ex TaqTM (Takara, Japan) with the specific primers in **Table 1**. The relative gene expression was normalized to β-actin.

Immunofluorescence

NRK-49F cells were cultured in 24-well plates with glass slides at a density of 2.5×10^4 cells/well. The cells were washed with phosphate-buffered saline (PBS) and fixed in 4% paraformaldehyde (Sigma-Aldrich) at 4˚C for 20 min. The specimens were washed with PBS, and the substrate was blocked with 2% bovine serum albumin in PBS for 1 h at room temperature. Immunofluorescence staining was performed using anti-α-SMA (dilution 1:200) or anti-fibronectin (1:400) at 4˚C overnight. After washing with PBS containing 0.02% Tween 20, the cell preparations were incubated with Alexa Fluor 555 goat anti-rabbit IgG (1:500) or Alexa Fluor 488 goat anti-rabbit IgG (1:500; CST). Images were taken using a Carl Zeiss LSM710 confocal microscope and processed using Photoshop software (Adobe Systems, Inc., San Jose, CA, United States). All of the images were quantified with ImageJ software and normalized to the respective control.

Statistical analysis

All data are expressed as the means ± S.E. Group comparisons were made with an analysis of variance (ANOVA) followed by the LSD test to identify differences among various groups. All data were analyzed using SPSS 18.0 software for Windows. $P < 0.05$ was considered to indicate a statistically significant difference.

RESULTS

SSB2 alleviated renal interstitial fibrosis in UUO mice

We investigated the potential effects of SSB2 in regulating renal fibrosis using the UUO model (Fig.2A), a classic model of renal interstitial fibrosis characterized by myofibroblast activation.

Evidence from the H&E staining revealed marked epithelial cell necrosis, inflammatory cell infiltration, tubular dilation and atrophy associated with interstitial fibrosis in the obstructed kidney tissues, and SSB2 administration significantly alleviated renal tubular injury and reduced total collagen deposition (Fig.2B). The total collagen deposition determined by Masson Trichrome and Sirius Red staining was more severe in the UUO group compared with the sham group (Fig.2B). After SSB2 administration, renal tubular injury was significantly alleviated and the total collagen deposition was reduced (Fig.2B, C). The 30 mg/kg + UUO group and 5 mg/kg CPN + UUO group exhibited more effectively reduced collagenous fiber induced by UUO compared with the 15 mg/kg + UUO group (Fig. 2B, C and D). Furthermore, compared with the sham group, the protein expression levels of α-SMA, which is a marker of myofibroblasts, and a major interstitial matrix protein fibronectin were significantly increased in UUO kidneys (Fig. 2E, F), whereas they were significantly decreased by the SSB2 and CPN treatment. In addition, the mRNA levels of α-SMA, collagen I and fibronectin were significantly upregulated in UUO mice, and they were also decreased by SSB2 administration (Fig.2F). These findings suggest that SSB2 can alleviate UUO-induced RIF in mice. We further found that the protein and mRNA levels of Gli1 in the UUO group were significantly increased, and 30 mg/kg SSB2 and CPN administration could downregulate Gli1 protein and mRNA. These results indicate that SSB2 can alleviate the UUO-induced excessive ECM deposition and RIF, and the pharmacological effects had a correlation with the Hh signaling pathway.

SSB2 inhibited the activation of renal interstitial fibroblasts *in vitro*

In UUO kidneys, upregulated expression levels of Shh are primarily located around the tubules, and it targets renal interstitial fibroblasts and activates Gli1 (Zhou et al., 2014). We found that SSB2 could decrease the expression of Gli, which serves as the readout of the Hh signaling pathway in UUO mice. We further investigated the potential effects of SSB2 on renal interstitial fibroblasts using a cell model system with an activated Hh pathway. Normal rat kidney interstitial fibroblast NRK-49F cells were incubated with ShhN CM leading to upregulation of α-SMA, fibronectin and Gli1 at both the protein and mRNA levels (Fig. 3), representing the activation of the Hh pathway; myofibroblasts did so as well. Treatment with SSB2 attenuated the induction of these molecules dose-dependently. GDC0449 served as a positive inhibitor control for the Hh

signaling pathway. Images of immunofluorescence showed that 20 μM of SSB2 significantly decreased the product of α-SMA and fibronectin (Fig.4). These results demonstrated that SSB2 inhibits ECM accumulation in Hh-activated cells, supporting the results *in vivo* and indicating that inhibiting Hh activity may be an important molecular mechanism for SSB2 to decrease kidney fibrosis.

SSB2 inhibited the Hh signaling pathway selectively

To further investigate the effects of SSB2 on the Hh signaling pathway activity, we used Shh-CM to stimulate the activity of the Hh signaling pathway in NIH-3T3 cells. As shown in Fig.5 A, SSB2 reduced the mRNA expressions of Ptch1 and Gli1, the target transcriptional genes of transcriptional factor Gli1, reconfirming the inhibition effect on the Hh pathway. Concomitantly, SSB2 suppressed the Gli-luciferase reporter activity stimulated by Shh-CM in NIH-3T3 cells significantly in a dose-dependent manner, and the IC_{50} was 0.49 μM (Fig.5B). To exclude the possibility that SSB2 nonspecifically inhibited the Hh signaling pathway activity, we next examined the effects of SSB2 on several other signaling pathways, such as NF-κB activity stimulated by TNF-α in 293T cell and TCF/LEF activity stimulated by prostaglandin E2 (PGE2) in LS174T cell in Wnt signaling. As shown in Fig.5C and D, SSB2 failed to affect the NF-κB activity stimulated by TNF-α as well as the TCF/LEF activity in response to PGE2, whereas BAY11-7082 and H89, the positive inhibitor controls for the TNF-α/NF-κB and PGE2/TCF/LEF signaling pathways, respectively, significantly suppressing NF-κB and TCF/LEF activity. Hence, these data suggest that SSB2 possessed selectivity in suppressing Hh pathway activity.

SSB2 inhibited the Hh signaling pathway by acting on Smo

Having shown that SSB2 might specifically inhibit the Hh pathway, we set out to define the potential molecular target that SSB2 might act on. Using Gli2ΔN, which could cause permanent transcriptional activity of Gli2 (Roessler et al., 2005), we found that SSB2 did not affect the Gli-luciferase activity in NIH-3T3 cells expressing Gli2ΔN, whereas the Gli1 inhibitor JQ-1 significantly inhibited the response (Fig 6.A). This result suggests that SSB2 might act upstream of Gli in the Hh signaling pathway. Thereafter, Smo was a potent candidate because it had been tested in both a laboratory and clinical practice. The D473H mutation of Smo could aberrantly activate the Hh pathway and interfere with the blockage effect of the Hh pathway inhibitor

GDC0449, leading to drug resistance (Li et al., 2019). As shown in Figure 6 B, SSB2 failed to inhibit the Hh pathway induced by mutant Smo D473H. The same was true for GDC0449, whereas the downstream inhibitor JQ-1 functioned normally. In other words, the Smo mutation abolished the inhibition effect of SSB2, suggesting that Smo might be the molecular target of SSB2's inhibition effect in the Hh signaling pathway. Furthermore, the D473 amino acid was a critical site for SSB2 effects.

DISCUSSION

The present study provided evidence that SSB2, a bioactive component of triterpene saponins in *Bupleurum falcatum,* could alleviate renal fibrosis. *In vivo*, SSB2 was capable of alleviating renal tubular damage, interstitial fibrosis and prevented the deposition of ECM components of UUO mice. *In vitro*, SSB2 could also effectively inhibit myofibroblast activation and accumulation of ECM components. Furthermore, results indicated that the underlying mechanisms regarding the inhibitory effects of SSB2 may have been associated with inactivation of the hedgehog signaling pathway. The anti-fibrotic effect of SSB2 was mediated by inhibition of the Hh pathway, and Smo was the associated molecular target.

Increasing evidence suggests that the Hh signaling pathway interacts with several key signaling pathways and operates in a coordinated fashion during renal fibrogenesis. The Hh pathway plays a fundamental role in tissue patterning, cell growth and differentiation and kidney development, and its abnormal activation in the adult kidney results in progressive renal tubular atrophy and interstitial fibrosis (Cain and Rosenblum, 2011; Dai et al., 2009). Many studies have confirmed that activated Hh signaling is involved in fibrogenesis in the kidney (Fabian et al., 2012). The kidneys in Gli1-deficient mice are protected against the development of tubulointerstitial fibrosis after UUO (Ding et al., 2012; Rauhauser et al., 2015). In our study, SBB2 could downregulate both the mRNA and protein levels of Gli 1 in UUO kidneys, indicating that the anti-fibrotic effect of SSB2 might be associated with inhibition of the Hh signaling pathway.

Shh, one of three ligands for the Hh pathway, is a novel, inducible, tubule-derived growth factor that mediates epithelial-mesenchymal communication after kidney injury (Ding et al., 2012; Zhou et al., 2014). Shh is known to be expressed in epithelial cells during the development of several organs including the kidney, but it is mostly silenced in adult kidneys. Shh demonstrates its

10

biological activity through both autocrine and paracrine manners, and it transduces across the plasma membrane in the responding cells via either canonical or noncanonical pathways. Emerging evidence indicates that along with the progression of kidney injuries, hyperactive Shh signaling causes activation and proliferation of fibroblasts and matrix overproduction by multiple mechanisms, primarily via a mode of epithelial-mesenchymal interaction. Myofibroblasts are terminally differentiated cells responsible for the synthesis of interstitial ECM components. The process of fibroblast to myofibroblast transition during renal fibrosis is manifested by increased cell proliferation, α-SMA expression, augmented production of interstitial matrix, and loss of erythropoietin-producing capabilities. *In vitro*, human recombinant Shh protein could activate Ptch1 and Gli1 and induce α-SMA, desmin, Snail1, fibronectin, and collagen I expression (Ding et al., 2012; Zhou et al., 2014), suggesting a critical role for Shh signaling in regulating myofibroblast activation and matrix production. We used Shh-CM to activate Hh signaling and found that SSB2 could decrease the expression of fibronectin and α-SMA and the mRNA levels of Gli1 and Ptch1. Furthermore, we also found that Shh could promote fibroblast proliferation in cultured rat kidney and stimulate the induction of numerous proliferation-related genes (data not shown). These results indicate that the anti-fibrotic effect of SSB2 is associated with inhibition of the Hh signaling pathway.

In addition to the Shh signaling pathway, the TGF-β1, Wnt/β-catenin and Notch pathways are well recognized to play crucial roles in renal fibrosis in CKD. Pharmacological inhibition of NF-κB signaling has been shown to reduce kidney injury in the models of kidney fibrosis induced by folate or adenine overload (Kumar et al., 2015; Okabe et al., 2013), and the present study showed that SSB2 had no effect on the NF-κB signaling pathway. Small molecules that interfere with Wnt signaling also modulate the development of fibrosis (Dai et al., 2009), and we did not find that SSB2 could affect the Wnt/β-catenin signaling pathway either. Evidence (Bai et al., 2016; Lu et al., 2016) reveals crosstalk with the TGF-β and Hh signaling pathways in kidney injury, but no significant effect of SSB2 could be found in TGF-β1-induced activation of NRK49F cells. These data indicate that SSB2 selectively targets Hh signaling in kidney fibrosis.

The most common method of targeting the Hh pathway is through the manipulation of Smo activity because it is considered as the main signal transducer of this pathway. Smo is responsible

11

for a large variety of developmental processes. As the first member of a class of small molecular compounds that specifically inhibit the activity of Smo, cyclopamine has been utilized in the treatment of renal fibrosis, inhibiting fibroblast activation and matrix production, reducing matrix expression and mitigating fibrotic lesions after UUO and IRI (Ding et al., 2012; Zhou et al., 2014). We also proved that CPN can reduce matrix expression and mitigate fibrotic lesions *in vivo* (Fig.2). IPI-926, a more soluble and potent CPN derivative, did not attenuate renal fibrosis in UUO mice (Fabian et al., 2012), and these differences might be due to the chemical diversity of Smo modulators and their different pharmacological properties. In the present study, we demonstrated that SSB2 significantly suppressed Hh-driven activation in NRK-49F and NIH3T3 cells. However, SSB2 could not inhibit the Hh activity provoked by ectopic expression of Gli2ΔN, which had higher transcriptional activity compared with full-length Gli2 (Roessler et al., 2005), suggesting that SSB2 functions upstream of Gli and may act on Smo. The Smo D473H mutant receptor where an Asp-to-His point mutation was found in the Smo gene was refractory to inhibition by GDC-0449 due to loss of interaction between the drug and receptor (Metcalfe and de Sauvage, 2011). SSB2 might bind to Smo as an antagonist and have the same pharmacological effect as GDC0449. Further research will be conducted to identify whether SSB2 can attenuate fibrosis in other organs and act on Ptch1 or Shh in the Hh signaling pathway.

In conclusion, our study demonstrated that SSB2 could inhibit the Hh signaling pathway and reduce the accumulation of ECM components in the cortical interstitum. Furthermore, SSB2 might function by binding to Smo as an antagonist. These results implicate SSB2 as a potential therapeutic agent for the prevention of kidney fibrosis.

Authorship Contributions

The authors who participated in the research design were Xuemei Zhang, Cheng Nengneng and Hong Xin. Dadui Ren, Jia Luo, Yingxue Li and Jiahong Yang conducted experiments. Jing Zhang and Junqiu Liu performed the data analysis, and Dadui Ren, Xuemei Zhang and Hong Xin wrote or contributed to the writing of the manuscript.

Conflict of interest

The authors who have taken part in this study declare that they do not have anything to disclose regarding funding or conflicts of interest with respect to this manuscript.

REFERENCES

Bai, Y., Lu, H., Lin, C., Xu, Y., Hu, D., Liang, Y., Hong, W., Chen, B., 2016. Sonic hedgehog-mediated epithelial-mesenchymal transition in renal tubulointerstitial fibrosis. Int J Mol Med 37, 1317-1327.

Bowers, M., Eng, L., Lao, Z., Turnbull, R.K., Bao, X., Riedel, E., Mackem, S., Joyner, A.L., 2012. Limb anterior-posterior polarity integrates activator and repressor functions of GLI2 as well as GLI3. Dev Biol 370, 110-124.

Cain, J.E., Rosenblum, N.D., 2011. Control of mammalian kidney development by the Hedgehog signaling pathway. Pediatr Nephrol 26, 1365-1371.

Chen, L., Yang, T., Lu, D.W., Zhao, H., Feng, Y.L., Chen, H., Chen, D.Q., Vaziri, N.D., Zhao, Y.Y., 2018. Central role of dysregulation of TGF-beta/Smad in CKD progression and potential targets of its treatment. Biomed Pharmacother 101, 670-681.

Dai, C., Stolz, D.B., Kiss, L.P., Monga, S.P., Holzman, L.B., Liu, Y., 2009. Wnt/beta-catenin signaling promotes podocyte dysfunction and albuminuria. J Am Soc Nephrol 20, 1997-2008.

Decleves, A.E., Sharma, K., 2014. Novel targets of antifibrotic and anti-inflammatory treatment in CKD. Nat Rev Nephrol 10, 257-267.

Ding, H., Zhou, D., Hao, S., Zhou, L., He, W., Nie, J., Hou, F.F., Liu, Y., 2012. Sonic hedgehog signaling mediates epithelial-mesenchymal communication and promotes renal fibrosis. J Am Soc Nephrol 23, 801-813.

Fabian, S.L., Penchev, R.R., St-Jacques, B., Rao, A.N., Sipila, P., West, K.A., McMahon, A.P., Humphreys, B.D., 2012. Hedgehog-Gli pathway activation during kidney fibrosis. Am J Pathol 180, 1441-1453.

Kumar, D., Singla, S.K., Puri, V., Puri, S., 2015. The restrained expression of NF-kB in renal tissue ameliorates folic acid induced acute kidney injury in mice. PLoS One 10, e115947.

Kuntzen, T., Timm, J., Berical, A., Lennon, N., Berlin, A.M., Young, S.K., Lee, B., Heckerman, D., Carlson, J., Reyor, L.L., Kleyman, M., McMahon, C.M., Birch, C., Schulze Zur Wiesch, J., Ledlie, T., Koehrsen, M., Kodira, C., Roberts, A.D., Lauer, G.M., Rosen, H.R., Bihl, F., Cerny, A., Spengler, U., Liu, Z., Kim, A.Y., Xing, Y., Schneidewind, A., Madey, M.A., Fleckenstein, J.F., Park, V.M., Galagan, J.E., Nusbaum, C., Walker, B.D., Lake-Bakaar, G.V., Daar, E.S., Jacobson, I.M., Gomperts, E.D., Edlin, B.R., Donfield, S.M., Chung, R.T., Talal, A.H., Marion, T., Birren, B.W., Henn, M.R., Allen, T.M., 2008. Naturally occurring dominant resistance mutations to hepatitis C virus protease and polymerase inhibitors in treatment-naive patients. Hepatology 48, 1769-1778.

Lee, W.P., Lan, K.L., Liao, S.X., Huang, Y.H., Hou, M.C., Lan, K.H., 2019. Antiviral effect of saikosaponin B2 in combination with daclatasvir on NS5A resistance-associated substitutions of hepatitis C virus. J Chin Med Assoc 82, 368-374.

Li, Q.R., Zhao, H., Zhang, X.S., Lang, H., Yu, K., 2019. Novel-smoothened inhibitors for therapeutic targeting of naive and drug-resistant hedgehog pathway-driven cancers. Acta

Pharmacol Sin 40, 257-267.

Li, X.Q., Song, Y.N., Wang, S.J., Rahman, K., Zhu, J.Y., Zhang, H., 2018. Saikosaponins: a review of pharmacological effects. J Asian Nat Prod Res 20, 399-411.

Li, Y., Dai, C., Wu, C., Liu, Y., 2007. PINCH-1 promotes tubular epithelial-to-mesenchymal transition by interacting with integrin-linked kinase. J Am Soc Nephrol 18, 2534-2543.

Lu, H., Chen, B.C., Hong, W.L., Liang, Y., Bai, Y.H., 2016. Transforming growth factor-beta 1 stimulates hedgehog signaling to promote epithelial-mesenchymal transition after kidney injury. Febs Journal 283, 3771-3790.

Maity, T., Fuse, N., Beachy, P.A., 2005. Molecular mechanisms of Sonic hedgehog mutant effects in holoprosencephaly. Proc Natl Acad Sci U S A 102, 17026-17031.

Meran, S., Steadman, R., 2011. Fibroblasts and myofibroblasts in renal fibrosis. Int J Exp Pathol 92, 158-167.

Metcalfe, C., de Sauvage, F.J., 2011. Hedgehog fights back: mechanisms of acquired resistance against Smoothened antagonists. Cancer Res 71, 5057-5061.

Okabe, C., Borges, R.L., de Almeida, D.C., Fanelli, C., Barlette, G.P., Machado, F.G., Arias, S.C., Malheiros, D.M., Camara, N.O., Zatz, R., Fujihara, C.K., 2013. NF-kappaB activation mediates crystal translocation and interstitial inflammation in adenine overload nephropathy. Am J Physiol Renal Physiol 305, F155-163.

Rauhauser, A.A., Ren, C., Lu, D., Li, B., Zhu, J., McEnery, K., Vadnagara, K., Zepeda-Orozco, D., Zhou, X.J., Lin, F., Jetten, A.M., Attanasio, M., 2015. Hedgehog signaling indirectly affects tubular cell survival after obstructive kidney injury. Am J Physiol Renal Physiol 309, F770-778.

Robbins, D.J., Fei, D.L., Riobo, N.A., 2012. The Hedgehog signal transduction network. Sci

15

Signal 5, re6.

Roessler, E., Ermilov, A.N., Grange, D.K., Wang, A., Grachtchouk, M., Dlugosz, A.A., Muenke, M., 2005. A previously unidentified amino-terminal domain regulates transcriptional activity of wild-type and disease-associated human GLI2. Hum Mol Genet 14, 2181-2188.

Vilayur, E., Harris, D.C., 2009. Emerging therapies for chronic kidney disease: what is their role? Nat Rev Nephrol 5, 375-383.

Zeisberg, M., Neilson, E.G., 2010. Mechanisms of tubulointerstitial fibrosis. J Am Soc Nephrol 21, 1819-1834.

Zhao, Y., Feng, L., Liu, L., Zhao, R., 2019. Saikosaponin b2 enhances the hepatotargeting effect of anticancer drugs through inhibition of multidrug resistance-associated drug transporters. Life Sci, 116557.

Zhou, D., Li, Y., Zhou, L., Tan, R.J., Xiao, L., Liang, M., Hou, F.F., Liu, Y., 2014. Sonic hedgehog is a novel tubule-derived growth factor for interstitial fibroblasts after kidney injury. J Am Soc Nephrol 25, 2187-2200.

Table 1. Primers for reverse transcription-quantitative polymerase chain reaction analysis.

| Gene	Forward Primer Sequence (5'→3')	Reverse Primer Sequence (5'→3')
collagen 1 (mouse)	gctcctcttaggggccact	ccacgtctcaccattgggg
β-actin (mouse)	ggctgtattcccctccatcg	ccagttggtaacaatgccatgt
α-SMA (mouse)	gtcccagacatcagggagtaa	tcggatacttcagcgtcagga
fibronectin (mouse)	atgtggacccctcctgatagt	gcccagtgatttcagcaaagg
Gli 1 (mouse)	ccaagccaactttatgtcaggg	agcccgcttctttgttaatttga
Ptch1 (mouse)	aaagaactgcggcaagtttttg	cttctcctatcttctgacgggt
collagen 1 (rat)	gatcctgccgatgtcgctat	ggaggtcttggtggttttgtattc
β-actin (rat)	tatcctggcctcactgtcca	aagggtgtaaaacgcagctc
α-SMA (rat)	cctcatgccatcatgcgtct	ctcacgctcagcagtagtca
fibronectin (rat)	atgagaagcctggatcccct	cagttggggaagctcatctgt
Gli 1 (rat)	agcatgggaacagaaggacttt	agatggaaagagcccgcttc
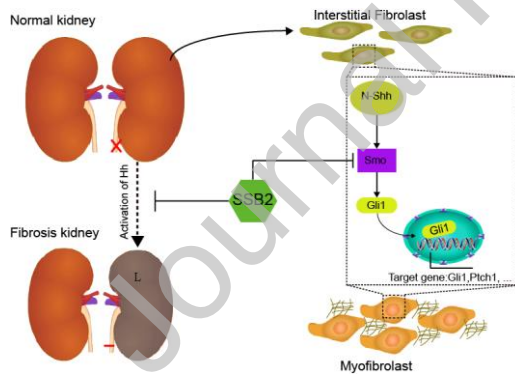
Graphical Abstract

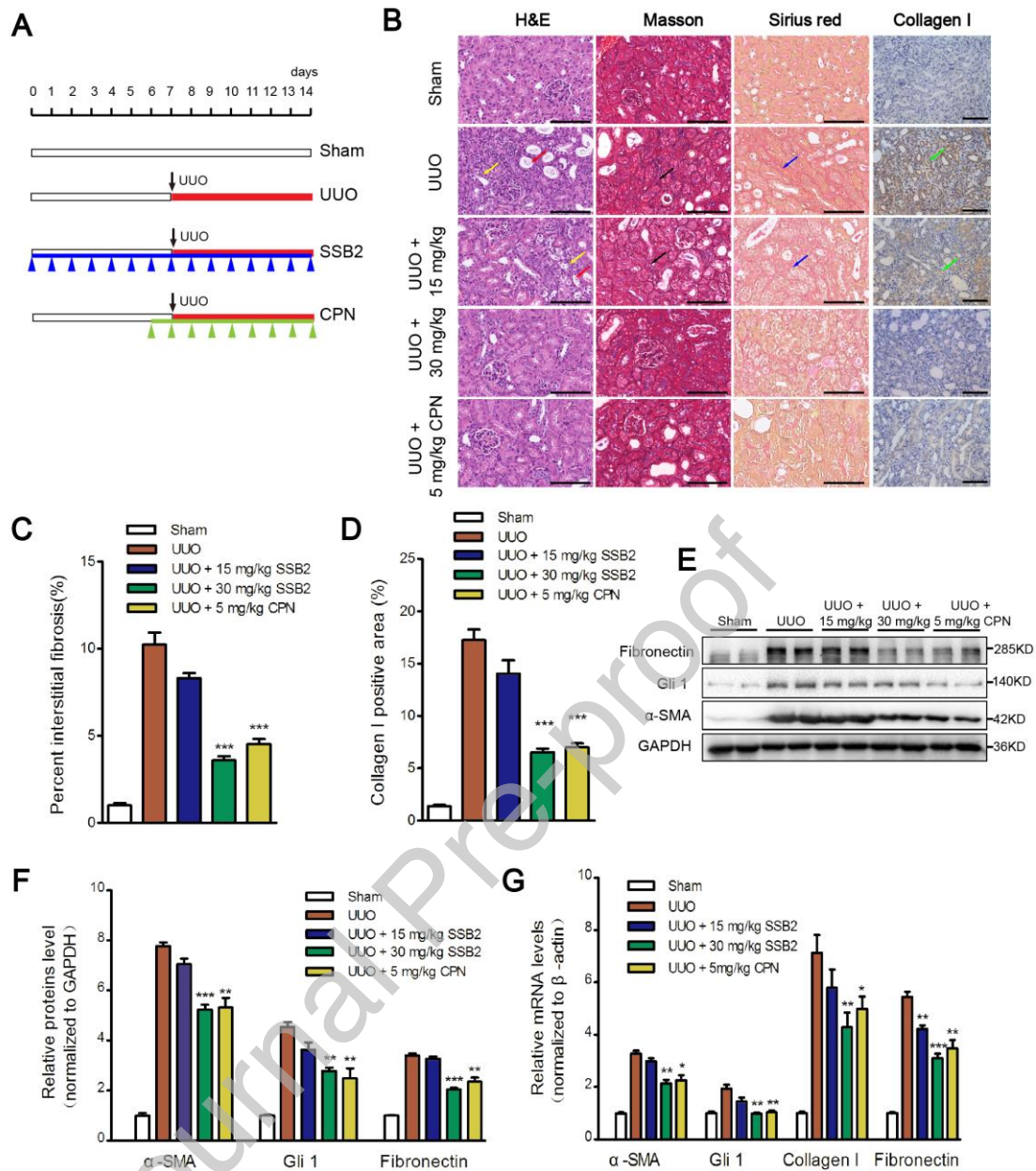17
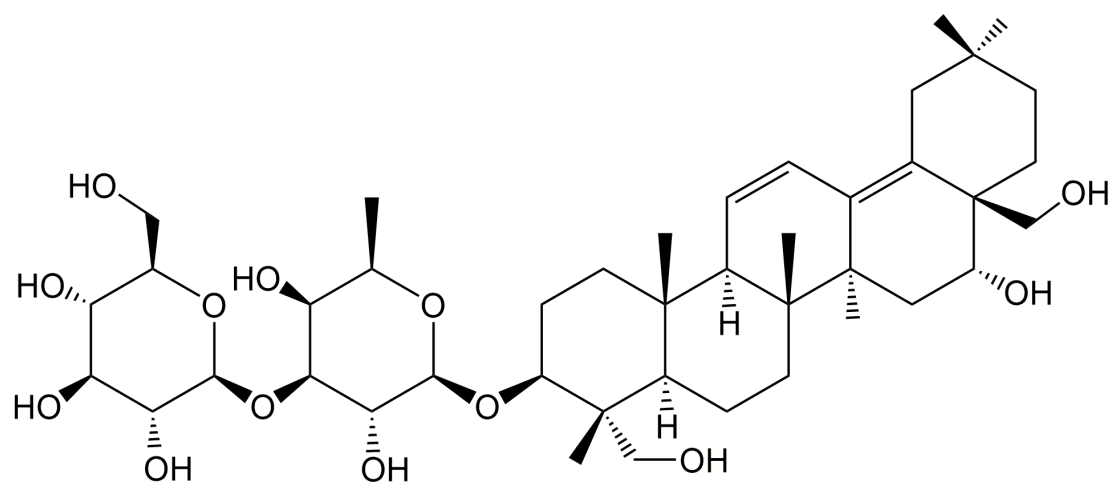
Figure 1. Chemical structure of SSB2.

Figure 2. SSB2 alleviated renal interstitial fibrosis in UUO mice. (A) A diagram for procedure of animal experiment. The mice were divided into the following five groups: sham, UUO, UUO + SSB2 (15 mg/kg), UUO + SSB2 (30 mg/kg) and UUO + CPN (5 mg/kg) and sacrificed on day 14. Blue arrowheads indicate the injection of SSB2 and green arrowheads indicate the application of CPN. (B) Histological and immunohistochemical staining of kidney sections isolated from UUO mice. Representative images of H&E, Masson Trichrome, Sirius red staining and IHC staining for collagen I showed SSB2 alleviated kidney injury and ECM accumulation induced by UUO. Yellow arrow indicates epithelial cell necrosis; red arrow indicates tubular dilation; black and blue arrow indicates fibrotic areas; green arrow indicates collagen I positive areas. Scale bar, 100 μm. (C) Renal interstitial fibrosis was evaluated by Masson staining in different animal groups. (D) Semi-quantitative analysis of immunohistochemistry staining for collagen I. (E) Representative Western blots showed SSB2 decreased the renal protein expressions of α-SMA, fibronectin and Gli1 in different

19

animal groups. (F) The relative intensity quantification of the bands in each group. (G) Real-time PCR analyses showed SSB2 downregulated the mRNA expression of collagen I, α-SMA, fibronectin and Gli1 induced by UUO in each group. Data are expressed as the mean ± S.E. *n* = 3, *P<0.05, **P<0.01, ***P<0.001 *vs*. UUO group.
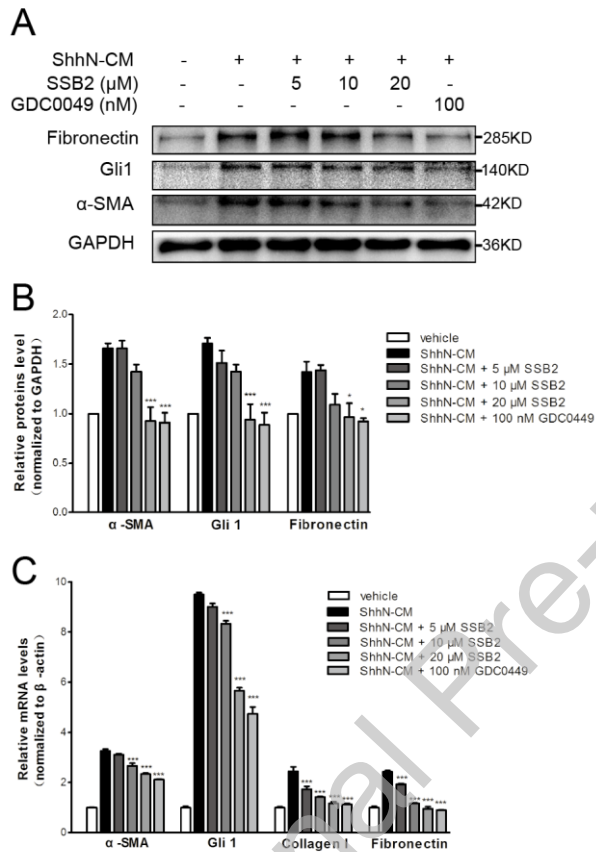

Figure 3. SSB2 suppressed hedgehog signaling and matrix production in ShhN-CM-treated NRK-49F cells. (A) Representative Western blots showed SSB2 decreased the protein expression of α-SMA, fibronectin and Gli1 in response to ShhN-CM which was used to active Hh pathway. NRK-49F cells were exposed to ShhN-CM containing various concentrations of SSB2 for 48 hours. GDC 0449 as a positive control. (B) The relative intensity quantification of the bands in each sample. (C) Real-time PCR analyses showed SSB2 downregulated the mRNA expression of α-SMA, Gli1, collagen I and fibronectin in response to ShhN-CM. NRK-49F cells were exposed to ShhN-CM containing various concentrations of SSB2 for 24 hours. ShhN-CM, conditioned medium containing ShhN protein, *n* = 3, *P<0.05, **P<0.01, ***P<0.001 *vs*. ShhN-CM group.
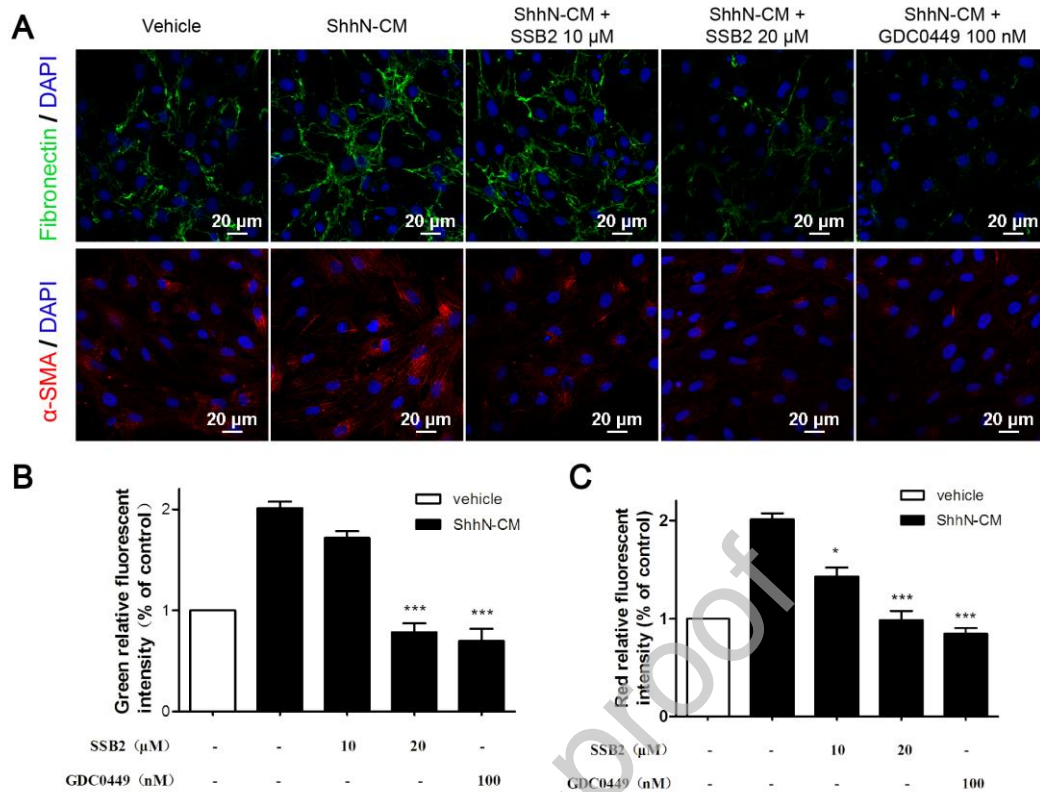
Figure 4. SSB2 inhibited NRK-49F cells activation and ECM accumulation. (A) Representative micrographs show that the SSB2 treatment decreased ShhN-CM-induced expression of fibronectin and α-SMA in NRK-49F cells. (B) The relative fluorescent intensity shows the quantification of fibronectin (green) and α-SMA (red) protein expression by immunofluorescence. Scale bar, 20 μm. $n = 3$, *$P<0.05$, ***$P<0.001$ *vs*. ShhN-CM group.
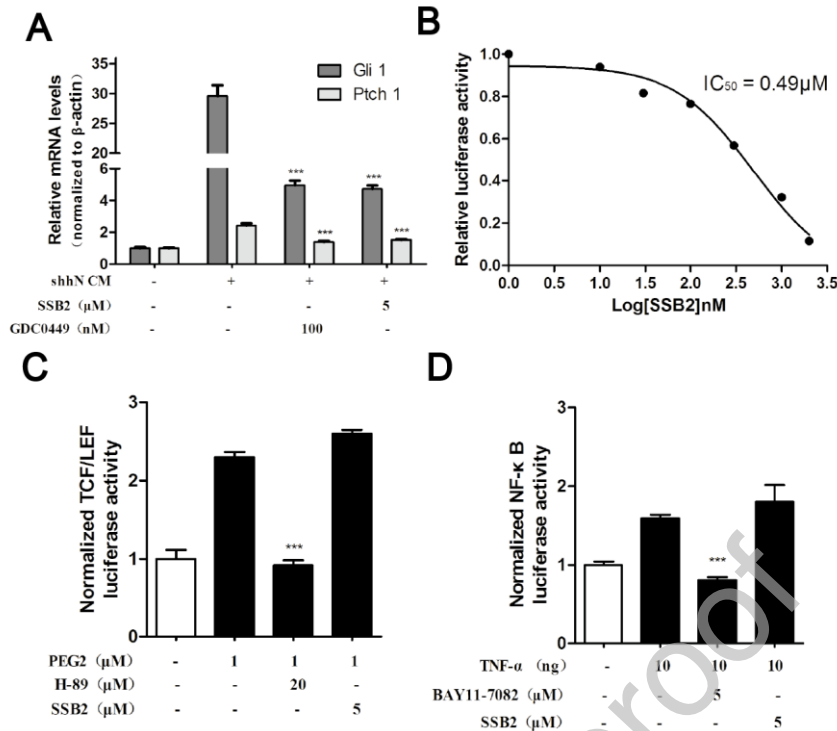
Figure 5. SSB2 selectively inhibited Hh pathway activity. (A) SSB2 suppressed the Gli1 and ptch1 mRNA expression in response to ShhN-CM in NIH-3T3 cells. *n* = 3, ****P*<0.001 *vs.* shhN-CM group. (B) Dose-response curve of inhibition effect of SSB2 on Gli-luciferase reporter activity stimulated by ShhN-CM. (C) SSB2 exhibited no effect on the TCF/LEF transcription activity in response to PGE2 in LS174T cells, H89 used as positive control. *n* = 3, ****P*<0.001 *vs.* PEG2 group. (D) SSB2 exhibited no effect on the NF-κB transcription activity in response to TNF-α stimulation in the 293T cells. BAY 11-872 used as positive control. *n* = 3, ****P*<0.001 *vs.* TNF-α group.
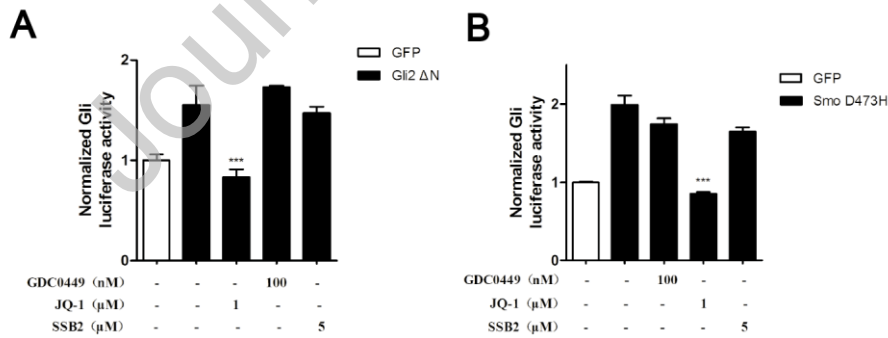

Figure 6. SSB2 inhibited the Hh signaling pathway activity by targeting Smo. (A) The dual luciferase reporter assay showed that SSB2 exhibited no effect on the Gli-luciferase activity in response to ectopic expression of Gli2ΔN. After transfected with Gli2ΔN, Gli-luciferase reporter, and the TK-Renilla constructs, NIH-3T3 cells were treated with SSB2, GDC0449 or JQ-1 for 24 h. GFP was used as a control. *n* = 3, ****P*<0.001 *vs.* vehicle. (B) Neither did SSB2 affect the Gli-luciferase activity in response to ectopic expression of Smo D473H which could induce aberrant activation of Hh pathway. GFP were used as a control. *n* = 3,

***P<0.001 *vs*. vehicle.

Supplementary Figure1. Histogram showing the percentage of the four cell lines viability. Cells was seeded in a 96-well plate at a density of about 5,000 cells/well and were treated with different concentrations of SSB2. Cell viability of 293T, LS174T and NIH3T3 cells were measured after 24 hours and NRK cells were measured after 48 hours by CCK-8 assay. $n = 3$, *$P < 0.05$, **$P < 0.01$, ***$P < 0.001$ *vs*. control group.